Dual-State Emission of an Engineered Photonics Oscillator: Advanced Nanostructures Emit at Multiple Spectrum

Prerna Chettri,[‡a,d] Anup Singhania,[‡a,d] Sudeshna Kalita,[a,d] Hidenobu Nakao,[b] Anirban Bandyopadhyay[*c] and Subrata Ghosh[*a,d]

[a]Natural Product Chemistry Group, Chemical Sciences & Technology Division, CSIR-North East Institute of Science & Technology, Jorhat-785006, Assam, India

[b]Hydrogen Related Materials Group, Hydrogen Technology Materials Field, Research Center for Energy and Environmental Materials (GREEN), National Institute for Materials Science (NIMS), 1-1 Namiki, Tsukuba, Ibaraki, 3050044 Japan

[c]International Center for Materials and Nanoarchitectronics (MANA) and Research Center for Advanced Measurement and Characterization (RCAMC), National Institute for Materials Science (NIMS), 1-2-1 Sengen, Tsukuba, Ibaraki-3050047, Japan

[d]Academy of Scientific and Innovative Research (AcSIR), Ghaziabad-201002, India

ABSTRACT. We've developed a molecular assembler, capable of crafting nanowires that exhibit programmable fluorescence across a broad spectrum of colors, yet in a precisely quantized manner. The assembler is a dendritic box of a 4th generation PAMAM dendrimer, P, doped it with Nile red fluoropore as controller C of PAMAM dynamics and N-terminals of PAMAM molecules are connected by double ratchet motors, M. Individual PCM assemblers have broad fluorescence band, but their self-assembled nanowires generate quantized cyan-green, yellow, and orange-red light emission in the spectra. PCM oscillators yield a versatile photonics applications like bio-imaging and energy harvesting. As nanowire modulates of photonic bandgaps causing a longer red shift in solid-phase PCM fluorophores that holds promise for drug delivery and cell separation like infra-red sensitive operations.

KEYWORDS. Dual-state emission, aggregation-induced emission, donor-acceptor, molecular motor, oscillator, dendrimer

1. Introduction

To achieve the emission of multiple colors from a single nanowire at different conditions, it is essential to consider the tunability and programming of the nanowire. This can be achieved through the use of nanowires with efficient second harmonic generation, acting as frequency converters, allowing the local synthesis of a wide range of colors via sum and difference frequency generation (Nakayama et al., 2007). Additionally, the use of nanowires with strong second harmonic generation response has been observed, indicating the potential for achieving fluorescence at different color bands in a quantized manner (Rørvik et al., 2011). Furthermore, the ability to encode emission fluorescence enhancement in the structure of nanowires is of high relevance for achieving the emission of multiple colors from a single nanowire (Zhao et al., 2016).

It is important to note that the behavior of cells on vertical nanowire arrays can impact the emission of different light colors from a single nanowire. For instance, fibroblast behavior on vertical nanowire arrays has been shown to reduce cell motility and proliferation rate (Persson et al., 2013). Additionally, the ability to induce cells to disperse nickel nanowires via integrin-mediated responses promises to advance applications of magnetic nanoparticles in drug delivery and cell separation, which could be relevant for achieving the emission of multiple colors from a single nanowire (Sharma et al., 2015).

Achieving the emission of multiple colors from a single nanowire at different conditions requires the use of nanowires with efficient second harmonic generation, tunability, and programming capabilities. Additionally, understanding the behavior of cells on nanowire arrays is crucial for optimizing the emission of different light colors from a single nanowire. However, for an efficient multi-color emission, aggregation-induced emission (AIE) and dual-state emission (DSE) of fluorophore substances are needed for lowering bandwidth and making emission sharp. Currently, there are attempts to develop single fluorogen polymers that can emit multi-color fluorescence in the aggregate state to achieve color-tuneability of the systems.[21-23]AIE is a beneficial strategy for generating highly effective solid-state molecular luminescence without suffering losses in quantum yield (Wang et al., 2019). This phenomenon involves nonemissive or weakly emissive chromophores in solution exhibiting enhanced luminescence in the aggregated states (Tajima et al., 2019).

The mechanism of AIE is related to restricted intermolecular rotations in the aggregated state that limit the nonradiative energy decay pathways (Liow et al., 2017). Therefore, if some fluorophores have dynamics of molecular machines, then the interaction is tunable, and the system can have a prolonged lifetime profile (see supporting information, PCMS lifetime graph).[19,20] This molecular engineering will allow the complex interplay between excitons and charge transfer species in the solid state. PCM is a donor-acceptor (D-A) based engineered organic oscillator developed from PAMAM dendrimer (P), Nile red controller (C), and molecular motor (M). While designing our fluoropore, PCM (Figure 1a), we have attached molecular motors all around its surface. When

subjected to an electrocatalytic synthesis, PCM produces a white powdery solid (deposited from water) as shown in Figure 1b. The microstructure analysis of this powder was found to have resulted from an assembly of thread-like nanowires. The solid-state fluorescence analysis of these nanowires shows the prominent association of cyan-green, yellow, and orange-red light emission in the spectra. When multiple PCM would bind to form nanowire, molecular rotors of individual PCM molecules would face each other inside the nanowire.

In a multi-band emission, the system emits electromagnetic radiation through a range of wavelengths. Each band spectrum has distinct wavelengths, and each emission band can result from various intermolecular electronic processes in the fluorophores and their dynamics, too. AIE-based fluorophores have weak fluorescence in dispersion but exhibit strong emission in the aggregate state, overcoming the aggregation-caused quenching (ACQ) effect (Wang et al., 2015). Furthermore, AIE materials emit more efficiently while in an aggregated state or solid state (Wang 2022) rather than in a dispersed state (Zhang et al., 2013). Here, in PCM, the absence of the Nile red fluorophores (λ_{ex} 580 nm, λ_{em} 650 nm in aqueous solution) in the vacant dendritic core of P turns the entire molecule into oscillator PM (λ_{ex} 350 nm, λ_{em} 410 nm in aqueous solution). Our developed double ratchet motor (DRM)[34,35] is the molecular motor connected to the dendrimer's N-terminals. The DRM itself produces blue fluorescence and has been designed to perform at ambient conditions in both solid and solution states, whereas the motor-integrated PCM oscillator in the aqueous solution produces a long-range fluorescence band (λ_{ex} 340 nm, λ_{em} 430 nm), see Figure 1c. This characteristic broad emission band of PCM covers an extended spectrum from blue to red lights (360 – 700 nm), while none of its constituent molecules characteristically show such emission.

AIE molecules also demonstrate fluorescence emission in the aggregation state together with excellent dispersibility, high resistance to photobleaching, and biocompatibility (Ding et al., 2019). Additionally, AIE materials have been developed that emit with multiple bands both in the solution and aggregated state, which is rarely reported (Zhang et al., 2022). The AIE phenomenon has been considered an effective way to overcome the notorious ACQ effect (Xu et al., 2011).

Moreover, the opposite photophysical phenomenon, aggregation-caused quenching (ACQ), refers to the phenomenon where fluorophores exhibit reduced emission in the aggregated state compared to the dispersed state (Sun et al., 2023). The development of materials that realize high emission efficiency through ACQ-to-AIE transformation has been explored (Sun et al., 2023). The study of AIE and DSE of fluorophore substances has expanded the family of AIE-exhibiting fluorophores, opening up new possibilities for various applications in optoelectronics, materials science, and chemistry.

1.1. Emission bands of different fluorophores can overlap to generate new intermittent emission bands near their photophysical spectral overlaps

The primary condition of efficient energy transfer in the PCM based nanowire is the close overlapping of the D emission energy bands with the absorption energy bands of the A. We have described energy transmission pathway inside PCM.[Reference] However, designing a complex arrangement of D-A is possible where two or more different fluorophores have distinct excitation and emission bands, forming a resonance energy transfer network. Some fluorophore absorbs and emits energy from the triplet states at characteristic wavelengths

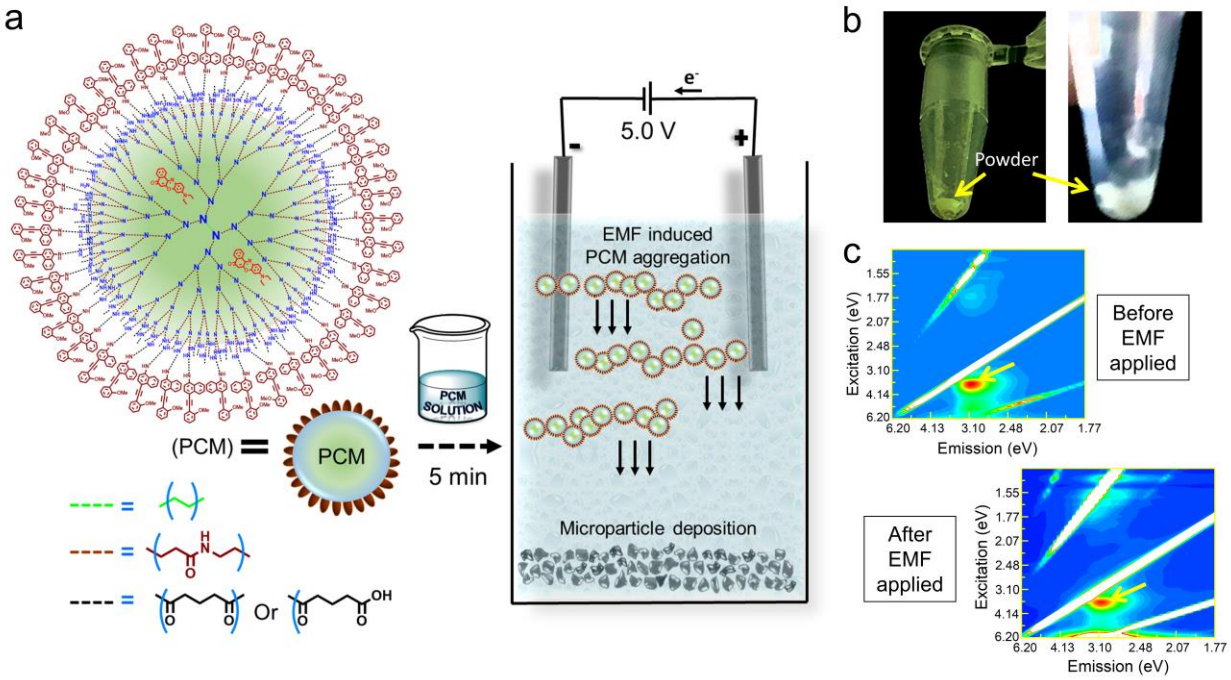

Figure 1. (a) Schematic representation of self-assembly of PCM under electrolysis condition (1.5 V for 10 min); (b) White powder of PCM nanowire; (c) CEES spectra of PCM architectures in aqueous solution before and after the self-assembly.

. Under certain conditions, the overlapping triplet state energies interact, forming new intermittent bands from where secondary emissions can occur.[15] This new emission band is distinguishable from the native emission bands of the individual fluorophores; generally, the new emission bands are found to be developed at the photophysical spectral overlapping zones. We demonstrate this in Figure 1c wherein, the separation between the newly evolved emission bands and the native emission bands of the individual fluorophores depends on the overlap of their spectral properties and energy transfer efficiency. The emission spectra combining process from different fluorophores can be used for various applications, including multiplexed detection and imaging.[16,17] It can provide valuable insights into interaction processes in biological events. Notably, the spectral overlaps of individual fluorophores may not depend on the distance of physical separation of the interacting fluorophores.[18]

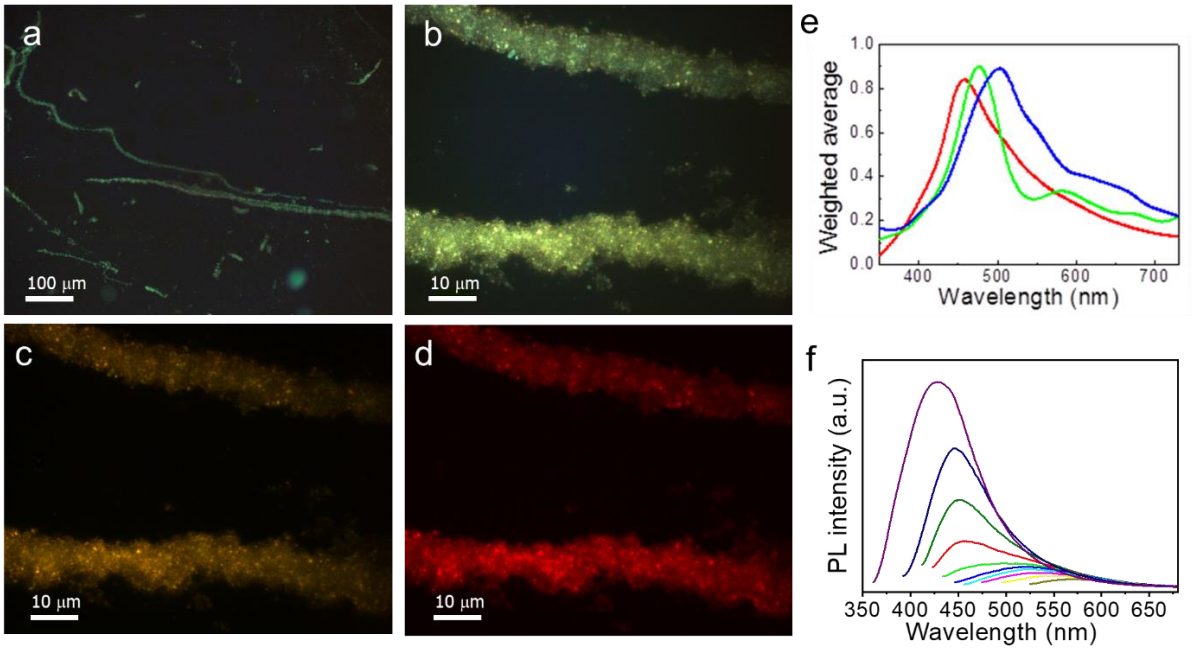

Figure 2. The four left panels (top and bottom) are 2D surface profiles of fluorescence images of nanowires. 2D emission profile at laser excitation frequency, 400 nm (green), (a) scale bar is 100 mm; (b) scale bar is 10 mm; (c) at laser excitation frequency, 470 nm (orange), scale bar is 10 mm; (d) and at laser excitation frequency, 539 nm (red), respectively; (e)Weighted average intensity at three nanowire lengths, 100 μm (red), 200 μm (green), and 300 μm (blue); (f) Photoluminescent spectra of PCM in aqueous solution.

2. Results & Discussion

2.1. Aggregation-induced dual-state emitting plasmon material from photonics oscillators

To further substantiate the aggregation-induced dual-state emitting possibility, we study the fluorescence spectra of individual PCM nanowires. As seen in the images (Figure 2), a nanowire responds positively to a number of light bands; however, the intensity varies with nanowire length. We can create clear optical images on these glass-coated films and store them for hours owing to the non-linear nature of the PCM nanowires, which is illustrated in Figure 2. As a result, films can be grown for real-time use. Excitation energy transfer substantially impacts molecular systems' optical and electrical properties. Automated production of massive structures would undergo a revolution if molecular machines and multi-level switching could accurately translate the work as intended in the PCM platform. According to our report, multiple dynamics are involved while creating a series of designs at different stages of self-assembly.[17] Although a previous stage produces the initial seed for the following stage, an inevitable energy-level transition manages the entire growth process. External control (electric field) and internal control (Nile red to DRM

interaction channel) interact more fluidly than only energy transmission-related dynamics. When a particular energy level transition is maintained across subsequent self-assemblies, the interaction's self-similarity provides a fractal growth structure visible in SEM or TEM (Figure 3).

2.2. Dual-state emission by DRM-connected spherical oscillators

The well-studied rotational feature of the motor, 4-((2-methoxyphenyl)ethynyl)naphthalen-1-amine, has been shown to have properties like a double ratchet motor (DRM).[34,35] The study of this motor's combined-excitation-emission spectroscopy (CEES) could validate the phenomenon through the associated characteristic emission properties.[39] More details about the mechanism of orbitals level interactions was further studied under a scanning tunneling microscope (STM).[40] The study also revealed that when multiple molecular motors were placed nearby, their power stroke (PS) units couple through resonance energy transfer. This information predicts that a combination of motors in a single platform would significantly influence the global emission of the system. The investigation was started by synthesizing PCM fluorophore by functionalizing PAMAM dendrimer with Nile red molecules and 4-((2-methoxyphenyl)ethynyl)naphthalen-1-amine molecules. The complete PCM structure becomes a spherical particle-like oscillator, and the electronic energy is transferred from one particle to another by non-radiative mechanisms known as excitation energy transfer. Such electronic energy transfers occur when two molecules are close, similar as seen in a dimer compound; one molecule's excited state interacts with another's ground state.[41] The contact can cause the organic molecules' excitation energies to change during this process, changing the system's overall absorption and emission spectra.

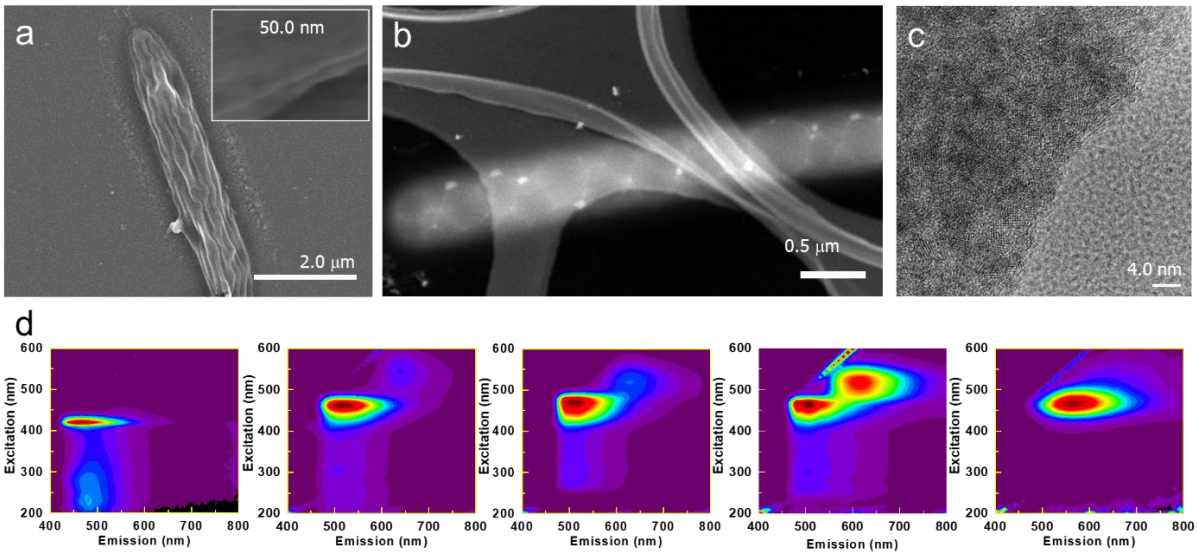

Figure 3. (a) SEM image (inset double helix edge); (b) TEM image; (c) TEM surface topology; (d)

Commonly, if fluorophore molecules show some induced aggregation upon some external or internal inducer effects; such aggregations generally follow J or H type aggregation and correspondingly result in solid-phase emitting materials known as aggregation-induced emitters; however, spherical fluorophores cannot join the J or H type aggregation. Therefore, instead of J or H type aggregation, a spherical molecule follows a close-packing aggregation pattern like ionic crystals.[42] According to Figure 3, in the present case, our PCM follows the close-packing aggregation and produces an aggregation-induced emission. A carrier transmission was observed along the nanowire length in a chain of motors in the supramolecular PCM. Thus, PCM holds the property of dual-state emission and response to multiple emission bands.

Our theoretical simulation suggests that the modulation of energy transmission distance (region of higher density in STM) determines the decay of the stabilized fluorescence states in the nanowires (see supporting material online). The oscillator strength, which measures a molecule's tendency to absorb or emit light, can also be propagated between the two molecules as the excitation energy transfers. Under various circumstances, spherical oscillators can self-assemble to produce superstructures of various orders and shapes (Figure 3a-c). Additionally, rather than J and H type aggregates, their spherical shape eases the formation of closely spaced packing. Therefore, there are astronomical possibilities for the site energy to vary in the monomer's complex and generate new plasmonic characteristics. Further, oscillator strength is redistributed proportionately to the monomers and shift of excitation energies. [43]

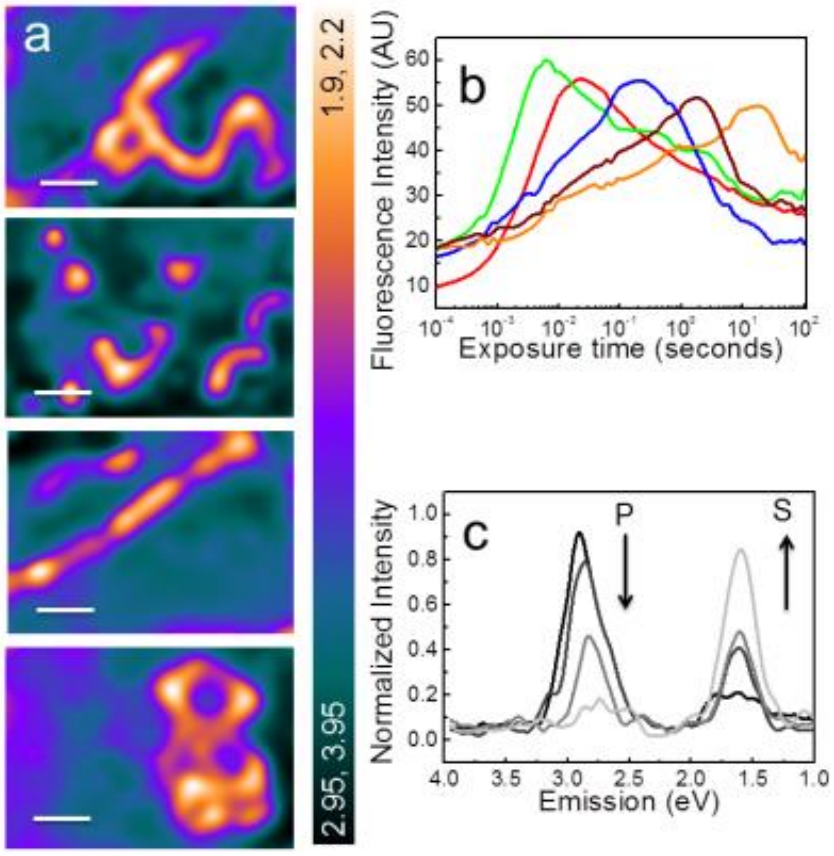

Figure 4. (a) PCM films dispersed in ethyl acetate on Si/SiO2, four images were written on film, corresponding fluorescence 2D profile to their right. Scale bar 100 nm, the vertical column is a scale for fluorescence colors. (b) Photoinhibition Kautsky plot fluorescence intensity vs. exposure time for Chlorophyll (red), others from left to right represent PCM films of four densities in panel a. (c) Response of PCMS film was studied by optically pumping the controller C at 3.10 eV, fluorescence intensity plotted at four intervals, within 800ns, P denotes peak for PAMAM and S denotes peak for Sensor.

The PAMAM-based encapsulation, coupled with the fluorophore interaction, enables the PCM supra structure to enhance the fluorescence stability for several orders of magnitude. The modulation of threshold intensity using the density of PCM is possible since the motors regulate the coupling in the nanowire. Therefore, we observe structure-independent features in the films described in Figure 4. We see four fluorescence scan images that are optically written, as demonstrated in Figure 4a. Thin films of PCM on a Si/SiO2 surface could be used reversibly to o-RAM and o-WORM not only one but pixel-by-pixel images on the same surface. One image is drawn, and the next is drawn after erasing the previous one. The 2D surface fluorescence profiles measured by pumping at peaks of M (2.8 eV) show that discrete spaces in the SEM appear joined, and the photonic superstructure is formed; thus, the DRMs, not only electronically but also optically couple in the PCM in the entire network. This could be the reason for its photostability. Now, we carry out a classical Kautsky-type photo inhibition experiment, as demonstrated in Figure 3b; we also plot the chlorophyll control to compare.

Interestingly, we could observe that we cannot edit the threshold exposure time in plant-based chlorophylls, which we can do by varying density distribution in a single PCM film. The role of super-clustering of photons is primary, as we find three orders of magnitude differences in the stability between isolated nanowires and their films. We could see the increasing stability of the emission of PCM compared to PM, where C is kept absent (Figure 5a-b). The length distribution is modulated by PCM density, leading to the clustering of fluorescence signals (Figure 5c).

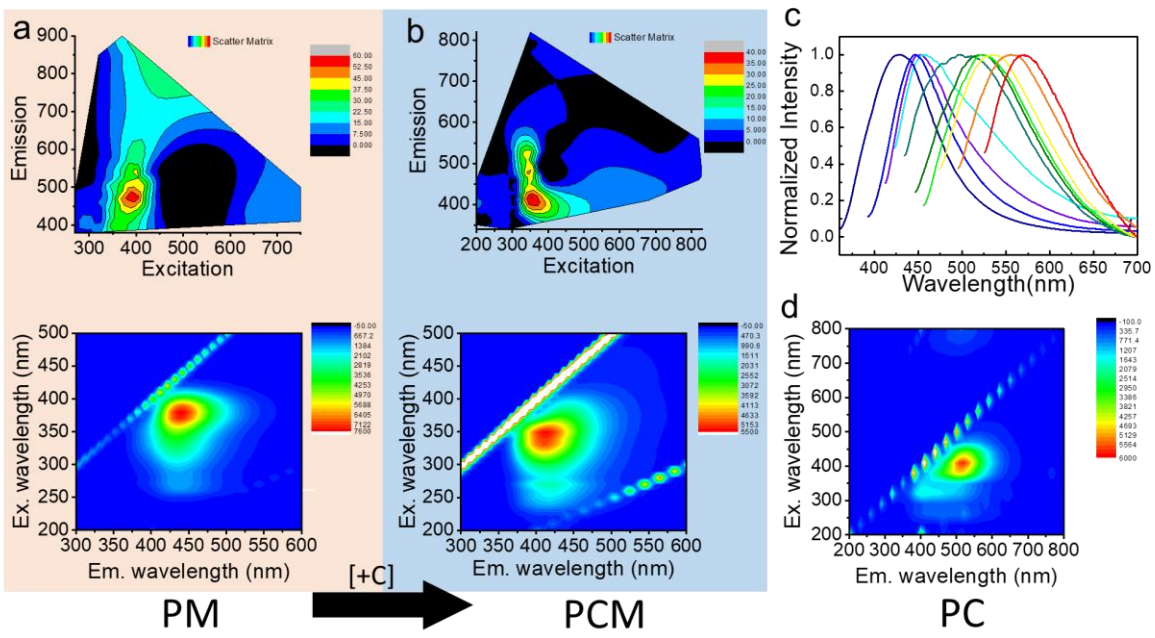

Figure 5. (a) DRM molecules with PAMAM dendrimer resulted in PM structure that has stable photoluminescence (PL) properties, the 2D spectrum of time scan emission profile, and PL intensity profile at various excitation-emission levels (panel a, top and bottom); (b) Controller molecules (C), Nile red with PM resulted in PCM structure that has dynamic PL properties, the 2D spectrum of time scan emission profile and PL intensity profile at various excitation-emission levels (panel b, top and bottom); (c) Normalized fluorescence emission wavelength distribution measured on the single nanowire;(d) The 2D spectrum of PL intensity profile of C encapsulated PAMAM dendrimer, PC at various excitation-emission levels.

For energy transfer, fractal seeds require a constant rule. In the future, fractal, energy level transition, and dynamics will be similarly correlated, and we can program much more sophisticated visible-size self-assembly. For further study, we advanced the PCM structure by including sensor molecules and produced PCMS. Transient optical pulses applied to the PCMS films at the absorption peaks of C (3.10 eV) and M (2.8 eV), one could observe that at first, the emission is at P (2.92 eV) and as a function of time, the emission peak at P decreases, and emission at S increases (Figure 4c). The complete activity changes from P to S; thus, the role of P as a buffer medium for the S→C→M loop is established. Both C and M are potentially equipped to inject noise into the energy trap cycle and is an important phenomenon to comprehend in fields such as photovoltaics, photochemistry, and materials science.

3. Conclusion

Encoding an energy transmission in the PCM is a generic tool since one could synthetically edit the loop complexity & single-state storage parameters by changing the number and nature of its

active components. Triggering a singular optical transition (here 2.15 eV↔2.90 eV) by eliminating noise would find remote applications in molecular robotics.20 We could draw an optical image on a chip several times and hold that image for several hours. This is an unprecedented optical information processing demonstrated in any system.

4. Experimental Section

Materials. All reagents and chemicals were purchased from commercial sources and used without further purification. Air and moisture-sensitive reactions were carried out in oven-dried sealed glassware under positive nitrogen pressure. NMR spectra were measured in Bruker Avance III 500 MHz and Jeol 400MHz FT-NMR Spectrometer. Photophysical properties were studied on HITACHI (U-3900) UV-Vis spectrophotometer and Horiba (Fluorlolog-3) fluorescence spectrophotometer.

Synthesis of PCM and PCMS. The PCM and PCMS was synthesized based on earlier reports.[19,20,36]

Self-assembly of PCM. A stock aqueous solution of PCM compound was prepared and further diluted it using Milli-Q. An electrocatalysis setup was prepared using a micro-cuvette & Sn electrode and filled it with dilute PCM solution. The dilute solution was added in microcuvette and 5 volt 'dc' current was passed through Sn electrode for 1-5 min. The white turbidity was collected at regular intervals, washed with isopropanol, centrifuged, sonicated, and further analyzed by different spectroscopic techniques.

Solid-state emission experiment: PCM sample was checked with fluorescent microscopy. Best images were obtained when the substrate was placed on a glass slide or a coverslip. Many long 1D structures in the direction of the electric field were also observed. For the use of a coverslip (thickness 0.1mm), an oil immersion lens can be applied to the sample. In addition, fluorescent images were also observed under various excitations. Experimentally, fluorescent spectra on microscopic areas on self-assembled dendrimer were measured. The collection volume for obtaining spectra was nearly diffraction-limited (1 μm^2).

Supporting Information.

~~All of the synthetic procedures of the PCM and LR(s), all additional NMR spectra of the compounds, absorption and emission spectroscopic data of the DRM and LR(s), theoretical studies, cyclic voltammograms.~~

AUTHOR INFORMATION

Corresponding Author

Subrata Ghosh − Chemical Sciences and Technology Division, CSIR-North East Institute of Science and Technology, Jorhat-785006, Assam, India; Academy of Scientific and Innovative

Research (AcSIR), Jorhat, Assam 785006, India; orcid.org/ 0000-0002-9104-517X; Email: ocsgin@gmail.com

Anirban Bandyopadhyay − International Center for Materials and Nanoarchitectronics (MANA) and Research Center for Advanced Measurement and Characterization (RCAMC), National Institute for Materials Science (NIMS), Tsukuba 305-0047, Japan; orcid.org/0000-0002-8823-4914; Email: anirban.bandyo@gmail.com

Present Addresses

Prerna Chettri− Chemical Sciences and Technology Division, CSIR-North East Institute of Science and Technology, Jorhat 785006, Assam, India; Academy of Scientific and Innovative Research (AcSIR), Jorhat, Assam 785006, India.

Anup Singhania − Chemical Sciences and Technology Division, CSIR-North East Institute of Science and Technology, Jorhat 785006, Assam, India; Academy of Scientific and Innovative Research (AcSIR), Jorhat, Assam 785006, India

Sudeshna Kalita− Chemical Sciences and Technology Division, CSIR-North East Institute of Science and Technology, Jorhat 785006, Assam, India; Academy of Scientific and Innovative Research (AcSIR), Jorhat, Assam 785006, India.

XX

Author Contributions

‡P.C. and A.S. contributed equally to this work.

Notes

The authors declare no competing financial interest.

ACKNOWLEDGMENT

The authors acknowledge SERB Government of India for Grant ECR/2016/001534 (2017-2020), and acknowledge the Asian office of Aerospace & D (AOARD), a part of the United States Air Force (USAF) for Grant FA2386-16-1-0003 (2016−2019). The authors thank CSIR-NEIST and NIMS Sengen-site for providing the necessary utilities and support. PC and SK are thankful to their PhD fellowship Grant 654/(CSIRNETJUNE2019) and 31/0025(12857)/2021-EMR-I respectively.

ABBREVIATIONS

DRM, double ratchet motor; PCM, P=PAMAM dendrimer, C=Controller, M=Double Ratchet Motor; AIE aggregation-induced emission; STM, scanning tunneling microscope;

REFERENCES

References:

Nakayama, Y., Pauzauskie, P., Radenović, A., Onorato, R., Saykally, R., Liphardt, J., … & Yang, P. (2007). Tunable nanowire nonlinear optical probe. Nature, 447(7148), 1098-1101. https://doi.org/10.1038/nature05921

Persson, H., Køber, C., Mølhave, K., Samuelson, L., Tegenfeldt, J., Oredsson, S., … & Prinz, C. (2013). Fibroblasts cultured on nanowires exhibit low motility, impaired cell division, and dna damage. Small, 9(23), 4006-4016. https://doi.org/10.1002/smll.201300644

Rørvik, P., Grande, T., & Einarsrud, M. (2011). One-dimensional nanostructures of ferroelectric perovskites. Advanced Materials, 23(35), 4007-4034. https://doi.org/10.1002/adma.201004676

Sharma, A., Orlowski, G., Zhu, Y., Shore, D., Kim, S., DiVito, M., … & Stadler, B. (2015). Inducing cells to disperse nickel nanowires via integrin-mediated responses. Nanotechnology, 26(13), 135102. https://doi.org/10.1088/0957-4484/26/13/135102

Zhao, X., Alizadeh, M., & Reinhard, B. (2016). Harnessing leaky modes for fluorescence enhancement in gold-tipped silicon nanowires. The Journal of Physical Chemistry C, 120(37), 20555-20562. https://doi.org/10.1021/acs.jpcc.5b11702

Ding, S., Che, Y., Yu, Y., Jia, D., & Zhao, J. (2019). Interactive aggregation-induced emission systems controlled by dynamic covalent chemistry. The Journal of Organic Chemistry, 84(11), 6752-6756. https://doi.org/10.1021/acs.joc.9b00495

Li, D. and Yu, J. (2016). Aiegens-functionalized inorganic-organic hybrid materials: fabrications and applications. Small, 12(47), 6478-6494. https://doi.org/10.1002/smll.201601484

Li, H., Guo, Y., Li, G., Xiao, H., Lei, Y., Huang, X., … & Cheng, Y. (2015). Aggregation-induced fluorescence emission properties of dicyanomethylene-1,4-dihydropyridine derivatives. The Journal of Physical Chemistry C, 119(12), 6737-6748. https://doi.org/10.1021/jp511060k

Liow, S., Zhou, H., Sugiarto, S., Guo, S., Chalasani, M., Verma, N., … & Loh, X. (2017). Highly efficient supramolecular aggregation-induced emission-active pseudorotaxane luminogen for functional bioimaging. Biomacromolecules, 18(3), 886-897. https://doi.org/10.1021/acs.biomac.6b01777

Sun, H., He, T., Zhang, C., Wang, S., Dong, L., Li, Z., … & Zhang, Q. (2023). Structural engineering of red luminogens to realize high emission efficiency through acq-to-aie transformation. Chemistry - A European Journal, 29(26). https://doi.org/10.1002/chem.202300029

Tajima, K., Fukui, N., & Shinokubo, H. (2019). Aggregation-induced emission of nitrogen-bridged naphthalene monoimide dimers. Organic Letters, 21(23), 9516-9520. https://doi.org/10.1021/acs.orglett.9b03699

Wang, H., Liu, G., Gao, H., & Wang, Y. (2015). A ph-responsive drug delivery system with an aggregation-induced emission feature for cell imaging and intracellular drug delivery. Polymer Chemistry, 6(26), 4715-4718. https://doi.org/10.1039/c5py00584a

Wang, L. (2022). Exactly opposite luminescence behaviors of aggregated diketopyrrolopyrrole derivatives depending on different molecular conformations. The Journal of Physical Chemistry C, 126(19), 8499-8510. https://doi.org/10.1021/acs.jpcc.2c01346

Wang, T., Su, X., Zhang, X., Nie, X., Huang, L., Zhang, X., … & Zhang, G. (2019). Aggregation-induced dual-phosphorescence from organic molecules for nondoped light-emitting diodes. Advanced Materials, 31(51). https://doi.org/10.1002/adma.201904273

Xu, B., Chi, Z., Li, H., Zhang, X., Li, X., Liu, S., … & Xu, J. (2011). Synthesis and properties of aggregation-induced emission compounds containing triphenylethene and tetraphenylethene moieties. The Journal of Physical Chemistry C, 115(35), 17574-17581. https://doi.org/10.1021/jp205525s

Zhang, X., Liu, H., Zhuang, G., Yang, S., & Du, P. (2022). An unexpected dual-emissive luminogen with tunable aggregation-induced emission and enhanced chiroptical property. Nature Communications, 13(1). https://doi.org/10.1038/s41467-022-31281-9

Zhang, X., Wang, S., Liu, M., Tao, L., & Wei, Y. (2013). Surfactant modification of aggregation-induced emission material as biocompatible nanoparticles: facile preparation and cell imaging. Nanoscale, 5(1), 147-150. https://doi.org/10.1039/c2nr32698a

1. Itoh, T. Fluorescence and Phosphorescence from Higher Excited States of Organic Molecules. *Chem. Rev.* **2012**, *112* (8), 4541–4568.

2. Ray, A.; Das, S.; Chattopadhyay, N. Aggregation of Nile Red in Water: Prevention through Encapsulation in β-Cyclodextrin. *ACS Omega* **2019**, *4* (1), 15-24.

3. Teo, W.; Caprariello, A. V.; Morgan, M. L.; Luchicchi, A.; Schenk, G. J.; Joseph, J. T.; Geurts, J. J.; Stys, P. K. Nile Red Fluorescence Spectroscopy Reports Early Physicochemical Changes in Myelin with High Sensitivity. *PNAS* **2021**, *118* (8), p.e2016897118.

4. Xia, Q.; Zhang, Y.; Li, Y.; Li, Y.; Li, Y.; Feng, Z.; Fan, X.; Qian, J.; Lin, H. A Historical Review of Aggregation-Induced Emission From 2001 to 2020: A bibliometric analysis. *Aggregate* **2022**, *3*, e152.

5. Mei, J.; L. C. Leung, N.; T. K. Kwok, R.; W. Y. Lam, J.; Tang, B. Z. Aggregation-Induced Emission: Together We Shine, United We Soar!. *Chem. Rev.* **2015,** *115* (21), 11718-11940.

6. Belmonte-Vázquez, J. L.; Amador-Sánchez, Y. A.; Rodríguez-Cortés, L. A.; Rodríguez-Molina, B. Dual-State Emission (DSE) in Organic Fluorophores: Design and Applications. *Chem. Mat.* **2021**, *33* (18), 7160-7184.

7. Zhang, Y.; Zhuo, P.; Yin, H.; Fan, Y.; Zhang, J.; Liu, X.; Chen, Z. Solid-State Fluorescent Carbon Dots with Aggregation-Induced Yellow Emission for White Light-Emitting Diodes with High Luminous Efficiencies. *ACS Appl. Mater. Interfaces* **2019,** *11* (27), 24395-24403.

8. Gierschner, J.; Shi, J.; Milián-Medina, B.; Roca-Sanjuán, D.; Varghese, S.; Park, S. Y. Luminescence in Crystalline Organic Materials: From Molecules to Molecular Solids. *Adv. Opt. Mater.* **2021**, *9*, 2002251.

9. Durko, M.; Ulrich, G.; Jacquemin, D.; Mysliwiec, J.; Massue, J. Solid-State Emitters Presenting a Modular Excited-State Proton Transfer (ESIPT) Process: Recent Advances in Dual-State Emission and Lasing Applications. *Phys. Chem. Chem. Phys*. **2023**, *25*, 15085-15098.

10. Rodríguez-Cortés, L. A.; Navarro-Huerta, A.; Rodríguez-Molina, B. One Molecule to Light it All: The Era of Dual-State Emission. *Matter* **2021**, *4* (8), 2622-2626.

11. Woods, J. F.; Gallego, L.; Pfister, P.; Maaloum, M.; Jentzsch, A. V.; Rickhaus, M. Shape-assisted self-assembly. *Nat. Commun.* **2022**, 13, 3681.

12. Roy Chowdhury, S.; Nandi, S. K.; Podder, D.; Haldar, D. Conformational Heterogeneity and Self-Assembly of α,β,γ-Hybrid Peptides Containing Fenamic Acid: Multistimuli-Responsive Phase-Selective Gelation. *ACS Omega* **2020**, 5 (5), 2287–2294.

13. Sarkar, D.; Ghosh, S.; Venkateswaran, R. V. A Biomimetic Type Expedient Approach to the Tricyclic Core of Xyloketals. Application to a Short, Stereocontrolled Synthesis of Alboatrin and a Remarkable Epi to Natural Isomerization. *Tetrahedron Lett.* **2009**, 50 (13), 1431-1434.

14. Clapp, A. R.; Medintz, I. L.; Mauro, J. M.; Fisher, B. R.; Bawendi, M. G.; Mattoussi, H. Fluorescence Resonance Energy Transfer Between Quantum Dot Donors and Dye-Labeled Protein Acceptors. *J. Am. Chem. Soc.* **2004**, *126* (1), 301-310.

15. Ehrler, B.; Yanai, N.; Nienhaus, L. Up- and down-conversion in molecules and materials. *J. Chem. Phys.* **2021**, *154*, 070401,

16. Mehta, S.; Zhang, Y.; Roth, R.H.; Zhang, J.-f.; Mo, A.; Tenner, B.; Huganir, R. L.; Zhang, J. Single-fluorophore biosensors for sensitive and multiplexed detection of signalling activities. *Nat. Cell Biol.* **2018**, *20*, 1215–1225.

17. Li, B.; Zhao, M.; Zhang, F. Rational Design of Near-Infrared-II Organic Molecular Dyes for Bioimaging and Biosensing. *ACS Materials Lett.* **2020**, *2*, 905–917.

18. Li, K.; Xu, S.; Xiong, M.; Huan, S. Y.; Yuan, L.; Zhang, X. B. Molecular Engineering of Organic-Based Agents for in-situ Bioimaging and Phototherapeutics. *Chem. Soc. Rev.* **2021**, *50* (21), 11766-11784.

19. Ghosh, S.; Fujita, D.; Bandyopadhyay, A. An Organic Jelly Made Fractal Logic Gate with An Infinite Truth Table. *Sci. Rep.* **2015**, *5*, 11265.

20. Ghosh, S.; Dutta, M.; Sahu, S.; Fujita, D.; Bandyopadhyay, A., 2014. Nano Molecular-Platform: A Protocol to Write Energy Transmission Program inside a Molecule for Bio-Inspired Supramolecular Engineering. *Adv. Fun. Mat.* **2014**, *24* (10), 1364-1371.

21. Gouthaman, S.; Jayaraj, A.; Sugunalakshmi, M.; Sivaraman, G.; Swamy P, C. Supramolecular self-assembly mediated aggregation-induced emission of fluorene-derived cyanostilbenes: multifunctional probes for live cell-imaging *J. Mater. Chem. B.* **2022**, *10*, 2238-2250.

22. Wang, Q.; Zhang, Q.; Zhang, Q. –W.; Li, X.; Zhao, C. –X.; Xu, T.-Y.; Qu, D.-H.; He, T. Color-Tunable Single-Fluorophore Supramolecular System with Assembly-Encoded Emission. *Nat. Comm.* **2020**, *11*, 158.

23. Dihua, D.; Li, Z.; Yang, J.; Wang, C.; Wu, J. –R.; Wang, Y.; Zhang, D.; Yang, Y. -W. Supramolecular Assembly-Induced Emission Enhancement for Efficient Mercury(II) Detection and Removal. *J. Am. Chem. Soc.* **2019**, *141*(11), 4756–4763.

24. Qiu, C. –W.; Odom, T. W. Introduction: Chemistry of Metamaterials. *Chem. Rev.* **2022**, *122*(19), 14987–14989.

25. Karawdeniya, B. I.; Damry, A.M.; Murugappan, K.; Manjunath, S.; Bandara, Y. N. D.; Jackson, C. J.; Tricoli, A.; Neshev, D. Surface functionalization and texturing of optical metasurfaces for sensing applications. *Chem. Rev.* **2022,** *122* (19), 14990-15030.

26. Guan, J., Park, J. E., Deng, S., Tan, M.J., Hu, J. and Odom, T.W. Light–matter interactions in hybrid material metasurfaces. *Chem. Rev.* **2022**, *122* (19), 15177-15203.

27. Zheludev, N.; Kivshar, Y. From Metamaterials to Metadevices. *Nat. Mat.* **2012**, *11*, 917–924.

28. Xu, X.; Peng, B.; Li, D.; Zhang, J.; Wong, L. M.; Zhang, Q.; Wang, S.; Xiong, Q. Flexible Visible–Infrared Metamaterials and Their Applications in Highly Sensitive Chemical and Biological Sensing. *Nano lett.* **2011**, *11*(8), 3232-3238.

29. Fainberg, B. D.; Rosanov, N. N.; Veretenov, N. A. Light-Induced "Plasmonic" Properties of Organic Materials: Surface Polaritons and Switching Waves in Bistable Organic Thin Films. *Appl. Phys. Lett.* **2017**, *110* (20), 203301.

30. Wang, P.; V. Krasavin, A.; Liu, L.; Jiang, Y.; Li, Z.; Guo, X.; Tong, L.; V. Zayats, A.; Molecular Plasmonics with Metamaterials. *Chem. Rev.* **2022**, *122*, 15031–1508.

31. Lee, S.; Sim, K.; Moon, S. Y.; Choi, J.; Jeon, Y.; Nam, J. M.; S. J., Park. Controlled Assembly of Plasmonic Nanoparticles: From Static to Dynamic Nanostructures. *Adv. Mat.* ***2021***, 3*3* (46), 2007668.

32. Busch, K.; Lölkes, S.; Wehrspohn, R. B.; Föll, H. Photonic Crystals: Advances in Design, Fabrication, and Characterization. 2006. John Wiley & Sons.

33. Moon, J. H.; Yang, Shu Chemical Aspects of Three-Dimensional Photonic Crystals. *Chem. Rev.* **2010**, *110*, 547–574.

34. Singhania, A.; Ghosh, I.; Sahoo, P.; Ghosh, S., Bandyopadhyay. A. Radio Waveguide-Rotors Work in Unison on a Single Surface Converts Heat into Power. *Nano Lett.* **2020**, *20*, 6891–6898.

35. Singhania, A.; Chatterjee, S.; Kalita, S.; Saha, S.; Chettri, P.; Gayen, F. R.; Saha, B.; Sahoo, P.; Bandyopadhyay A., Ghosh, S. An Inbuilt Electronic Pawl Gates Orbital Information

Processing and Controls the Rotation of a Double Ratchet Rotary Motor. *ACS Appl. Mater. Interfaces* **2023**, *15*, 15595-15604.

36. Ghosh, S.; Dutta, M.; Ray, K.; Fujita, D.; Bandyopadhyay, A. Simultaneous One Pot Synthesis of Two Fractal Structures via Swapping Two Fractal Reaction Kinetic States. *Phys. Chem. Chem. Phys.* **2016***, 18,* 14772-14775.